Translational Diffusion on Heterogeneous Lattices: A Model for Dynamics in Glass Forming Materials

Marcus T. Cicerone,[†] Paul A. Wagner,[‡] and M. D. Ediger*

Department of Chemistry, University of Wisconsin−Madison, 1101 University Avenue, Madison, Wisconsin 53706

Received: February 17, 1997; In Final Form: April 8, 1997[⊗]

Simulations of translational motion on lattices with spatially heterogeneous dynamics have been performed. Translation occurs by nearest neighbor jumps on a three-dimensional simple cubic lattice. The overall lattice is subdivided into cubic blocks. The rate for jumps within a given block is controlled by the local relaxation time (or rotation time) for that block. Blocks exchange their local relaxation times on a specified time scale. If the local distribution of relaxation times is given by a Kohlrausch−Williams−Watts distribution, the simulation results can reproduce experimental observations of enhanced translational diffusion in supercooled liquids. This adds further weight to arguments that dynamics in deeply supercooled liquids are spatially heterogeneous and that this heterogeneity is responsible for the non-exponential relaxation functions which are often observed. For systems with only two local relaxation times, the simulation results are in good agreement with effective medium theory.

I. Introduction

While systematic studies of the glass transition and the properties of supercooled liquids began at least 7 decades ago, the past decade has seen a resurgence of interest in these problems.[1−3] One long-standing observation is that relaxation processes in supercooled liquids are often characterized by non-exponential relaxation functions.[4] For example, if one fits data to the Kohlrausch−Williams−Watts (KWW) or stretched exponential function,

$$\mathrm{CF}(t) = \mathrm{e}^{-(t/\tau)^{\beta}} \tag{1}$$

β values near 0.5 are often observed near the glass transition temperature T_g. Non-exponential relaxation functions can be interpreted in two different ways.[5] One can imagine that a heterogeneous set of environments exists in a supercooled liquid; relaxation in a given environment is nearly exponential, but the relaxation time varies significantly among environments. Alternatively, one can imagine that supercooled liquids are homogeneous and that each molecule relaxes nearly identically in an intrinsically non-exponential manner. Very recent experiments have shown that spatially heterogeneous dynamics are at least partially responsible for non-exponential relaxation functions near T_g.[6−10]

Spatially heterogeneous dynamics have also been implicated in recent observations of enhanced translational diffusion in supercooled liquids. In several low-molecular weight supercooled liquids (e.g., *o*-terphenyl[11],[12] and trisnaphthylbenzene[13,14]), self-diffusion or diffusion of a probe similar in size to the host molecule has been reported to have a temperature dependence significantly weaker than the viscosity. In contrast, in the same systems, rotational motion has essentially the same temperature dependence as the viscosity. The model independent interpretation of these results is that molecules translate further and further per rotational correlation time as the temperature is lowered toward T_g. Thus, translational diffusion is "enhanced" relative to rotational motion. This enhancement can be more than 2 orders of magnitude for low-molecular weight supercooled liquids.[11,13,15,16] For polymeric glass formers, translational diffusion of probes of various sizes can be enhanced more than 4 orders of magnitude.[17−19]

In this paper, we report simulations which determine how translational diffusion averages over spatial heterogeneity for a variety of cases potentially relevant to supercooled liquids.[20] These simulations have been performed to test whether the experimental observations of enhanced translational diffusion can be quantitatively explained by a simple model of spatially heterogeneous dynamics. We would like to understand, for example, how heterogeneous the dynamics would have to be in order to reproduce the experimental results. In the remainder of this section, we present background information which provides context for these simulations. First we explain the qualitative connection between enhanced translational diffusion and spatially heterogeneous dynamics. Then we present the experimental results which we wish to reproduce with our simulations. Finally we briefly explain our results.

How can spatially heterogeneous dynamics account for enhanced translational diffusion? We envision a system in which the dynamics in some regions of the sample are orders of magnitude faster than the dynamics in other regions perhaps 5 nm away. We assume that rotation and translation are locally coupled; i.e., a region in which molecules rotate unusually fast is also a region in which local translation is unusually fast. In such a heterogeneous system, translation and rotation experiments each average over the heterogeneity in their own way.[13,21] The orientation correlation function in such a system is a superposition of the orientation relaxation functions for the different regions of the sample. Molecules in more mobile regions relax quickly and are responsible for the fast initial decay in the correlation function, while molecules in less mobile regions give rise to a long tail in this function. Since the rotational correlation time is the integral of the correlation function, it weights regions of slower mobility to a much greater extent. In constrast, the long-time translational diffusion coefficient emphasizes regions of high mobility. Qualitatively, this is similar to a three-

* Author to whom correspondence should be addressed. E-mail address: ediger@chem.wisc.edu.

[†] Current address: Johnson and Johnson Clinical Diagnostics, Inc., 1999 Lake Ave., Rochester, NY 14650-2101.

[‡] Current address: Division of Chemistry and Chemical Engineering, California Institute of Techology, Pasadena, CA 91125.

[⊗] Abstract published in *Advance ACS Abstracts,* September 15, 1997.

S1089-5647(97)00595-6 CCC: $14.00

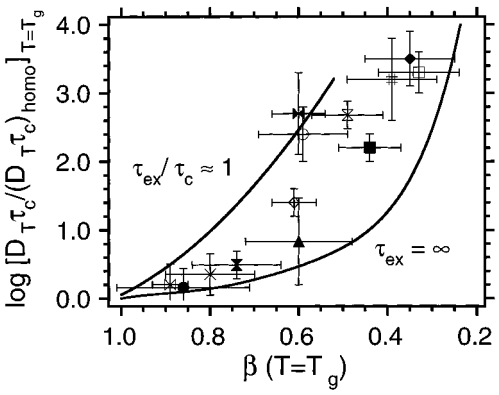

Figure 1. Correlation of enhanced translation ($D_T\tau_c$) with the KWW β parameter for probe rotation at T_g. The two lines are fits to simulation results for two different values of the exchange time. The data represent experimental results for tetracene/PIB (solid triangle); rubrene/PIB (solid circle); tetracene/polystyrene (solid diamond); rubrene/polystyrene (open diamond); BPEA/polystyrene (open circle); tetracene/polysulfone (open box); rubrene/polysulfone (solid box); rubrene/*o*-terphenyl (open bowtie); tetracene/*o*-terphenyl (solid bowtie); BPEA/*o*-terphenyl (×); anthracene/*o*-terphenyl (#); tetracene/trinaphthylbenzene (open hourglass); rubrene/trinaphthylbenzene (filled hourglass). Data taken from refs 11, 13, 17, 18, and 31.

dimensional network of resistors; most of the current follows paths of lower than average resistance. If the distribution of local relaxation times broadens as the temperature is lowered toward T_g, then translational motion will have a weaker temperature dependence than rotational motion.

If the above explanation is correct, both enhanced translational diffusion and the non-exponentiality of the rotational correlation function are a consequence of spatially heterogeneous dynamics, and a direct correlation should exist between these quantities. Figure 1 shows that this correlation does exist for experimental data from five supercooled liquids at their glass transition temperatures (experimental data shown as points with error bars). Here the KWW β parameter is used to characterize the non-exponentiality of the rotational correlation function. The product $D_T\tau_c$ characterizes the enhancement of translational diffusion (D_T is the translational diffusion coefficient, τ_c is the rotational correlation time). This product has been normalized by the value expected in a homogeneous environment.[22] Thus, one can read the vertical axis in Figure 1 as the number of orders of magnitude by which translational diffusion has been enhanced. The experimental data in Figure 1 provide strong support for the argument that enhanced translational diffusion is caused by spatially heterogeneous dynamics.

Figure 1 shows the experimental data which we have attempted to explain in our simulations of spatially heterogeneous systems. Our simulation algorithm produces all of the quantities needed to plot a point in this figure. Thus, we can ask what regions of parameter space, if any, produce results which are consistent with the experimental data shown in Figure 1. The two lines in the figure summarize our simulation results for two values of the exchange time τ_{ex} (the average length of time for which regions retain their dynamic identity). When τ_{ex} is infinite, the heterogeneity is static; i.e., a fast region always remains a fast region. While some of the experimental data are consistent with this limit, most of the data show a greater enhancement of translational motion. As τ_{ex} becomes shorter, translational motion becomes more enhanced for a given β value. The upper line in Figure 1 represents a set of simulations for the case when τ_{ex} is comparable to the rotational correlation time τ_c. Some of the data are only consistent with the model when $\tau_{ex}/\tau_c \approx 1$. Most of the experimental data are consistent with somewhat larger values of τ_{ex}/τ_c, perhaps as large as 6−10 or higher.

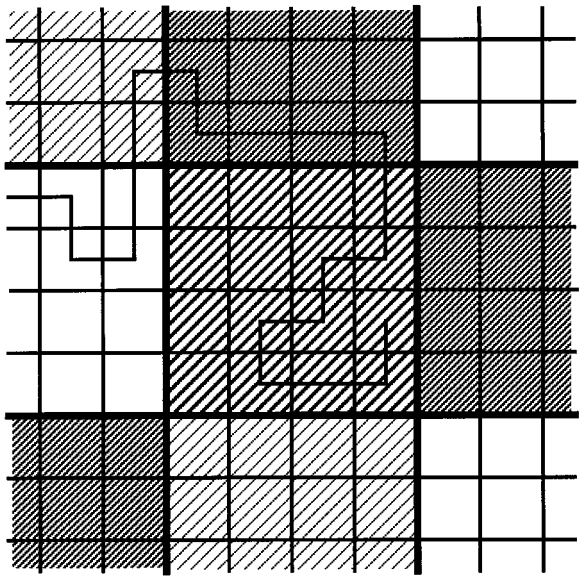

Figure 2. Schematic illustration of the model used in these simulations. Different levels of shading designate different local relaxation times.

II. Simulation Procedures

Model. Figure 2 is a schematic illustration of the model used in these simulations. Translational motion occurs by nearest neighbor jumps on a three-dimensional simple cubic lattice. The overall lattice is subdivided into cubic blocks. The rate for jumps within a given block is controlled by the local relaxation time (or rotation time) for that block. Within the interior of a block, the rules for translational motion are identical to those of a homogeneous system. Local relaxation times vary from block to block, as indicated schematically by different shading in Figure 2. Jumps between nearest neighbors in different blocks occur at a rate intermediate between the rates of jumps inside the two blocks. We assume that the probe solubility is uniform in space; i.e., the probe is equally likely to be found on any lattice site in the system. As specified below, the number of lattice sites per block and the number of blocks in the entire system is much larger than indicated in Figure 2.

Blocks do not necessarily retain their local relaxation times forever, but rather these are exchanged on the time scale of τ_{ex}. In contrast to some other approaches,[23,24] we choose τ_{ex} as an independent variable in order to make this simulation model as versatile as possible. For a given system, τ_{ex}/τ_c might be expected to decrease with increasing probe size. τ_{ex}/τ_c might be larger for a given probe if the matrix is a polymer instead of a low-molecular weight glass former. If the matrix were a phase separated polymer blend, τ_{ex}/τ_c might be extremely large. For completeness, in some simulations we consider the possibility that τ_{ex}/τ_c is much less than unity, although it is unclear what physical situation this describes.

Algorithm. Our simulation is defined by the following definitions and algorithm.

(1) k_{ij} is the rate constant for jumping from site i to site j; $k_{ij} = 0$ unless j is one of the six nearest neighbors of i.

(2) τ_{jump} is the average time required to jump from site i:

$$\tau_{jump} = \frac{1}{\sum_j k_{ij}} \qquad (2)$$

(3) When a jump occurs, the probability of jumping from i to j is

$$P_{ij} = \tau_{\text{jump}} k_{ij} \tag{3}$$

(4) t_{jump} is the actual time required for a given jump from site i; it is selected from a distribution such that $\langle t_{\text{jump}} \rangle = \tau_{\text{jump}}$ and the probability of remaining at position i decays exponentially.

(5) τ_{m} designates the local rotation time for the mth block. We set

$$\begin{aligned} k_{ij} &= 1/(18\tau_{\text{m}}) \qquad \text{if } i \text{ and } j \text{ are both in block } m \\ k_{ij} &= (1/18\tau_{\text{m}} + 1/18\tau_{\text{n}})/2 \qquad \text{if } i \text{ and j are in blocks } m \text{ and } n \end{aligned} \tag{4}$$

(6) $g(\tau)$ is the distribution function for the local rotation times. The probability of a given block having a certain τ is independent of the τ values of neighboring blocks.

(7) t_{ex} is the length of time for which the blocks retain their current dynamical states, i.e., after a time t_{ex} new τ values (chosen at random from $g(\tau)$) will be assigned to all blocks. t_{ex} is selected from a distribution such that $\langle t_{\text{ex}} \rangle = \tau_{\text{ex}}$ and the probability of selecting a particular t_{ex} decays as either an exponential or a stretched exponential (specified by β_{ex}).[25]

(8) After each step (or exchange process) in the simulation, a pseudorandom number is used to determine t_{jump} for the next step. If the dynamical states are not exchanged before this jump occurs, time will be incremented by t_{jump} and the new site will be recorded. A second random number is used to determine which of the six nearest neighbor sites is the destination of the jump (subject to the current probabilities P_{ij}). If the dynamical states are exchanged prior to the next scheduled jump, no jump occurs, time is incremented to the exchange time, a new t_{jump} is selected, and the process continues as described above. To illustrate this, t_1 is the last time the dynamical states were exchanged. At that time, the current value of t_{ex} was selected. t_2 ($>t_1$) is the last time a jump occurred. At that time, the current value of t_{jump} was selected. Two cases are possible: (a) If $t_1 + t_{\text{ex}} > t_2 + t_{\text{jump}}$, a jump occurs, the running time is incremented to $t_2 + t_{\text{jump}}$, and a new value of t_{jump} is selected. The value of t_2 is updated (to the current running time), and the process continues by again choosing option a or b. (b) If $t_1 + t_{\text{ex}} < t_2 + t_{\text{jump}}$, then no jump occurs, the running time is incremented to $t_1 + t_{\text{ex}}$, and new values of t_{ex} and t_{jump} are selected. The values of t_1 and t_2 are updated (to the current running time), and the process continues by again choosing option a or b. It is possible that the running time is incremented by multiple t_{ex} values without a jump taking place.

The algorithm described above is very efficient when $t_{\text{ex}} \gg t_{\text{jump}}$ since a step is taken each time two random numbers are selected. If $t_{\text{ex}} < t_{\text{jump}}$, many random numbers may be selected without taking a step. However, the inefficiency in this second case is balanced by the fact that much shorter trajectories are needed when this condition holds.

In these simulations, all blocks were cubic and contained the same number of lattice sites (typically $20 \times 20 \times 20$ or $40 \times 40 \times 40$). The overall simulation volume was also cubic, typically with 20 blocks on a side. Periodic boundary conditions were used on the overall lattice for simplicity, but the random walks were generally terminated before the root-mean-square displacement equaled the overall lattice size. Care was taken to ensure that the periodicity of the block structure had no effect on the results. Each simulation run typically averaged results from 100 to 1000 independent walks; typically a total of 10^9 steps were used for each simulation run. Mean-square displacements were calculated from the random walk trajectories using multiple starting points. Random errors in the reported diffusion coefficients are estimated to be $\leq 5\%$ unless otherwise indicated. Errors were estimated from the reproducibility of independent simulation runs. In all calculations in this paper, the lattice spacing is set to unity.

Test for a Homogeneous Lattice. For a homogeneous lattice, rules 1−5 above are known to be an exact solution to the diffusion equation; i.e., they produce $\langle r^2 \rangle$ proportional to t for all times.[26] We used this result to test rule 8. If τ is chosen to be unity in all blocks, then $\tau_{\text{jump}} = 3$, and for nearest neighbors, $k_{ij} = {}^1/_{18}$ and $P_{ij} = {}^1/_6$. Since $\langle r^2 \rangle = nl^2$ ($=n$ in our notation) for such a random walk, and $n = t/3$, then D_{T} is predicted to be ${}^1/_{18}$. This value was obtained in our simulations (within 1%) for choices of $\tau_{\text{ex}}/\tau_{\text{jump}}$ in the range from 0.03 to ∞. This result validates the algorithm for handling the interplay between t_{ex} and t_{jump}.

The numerical factor of ${}^1/_{18}$ used in the first part of rule 5 was chosen as follows. The Stokes−Einstein and Debye−Stokes−Einstein equations can be combined to give $D_{\text{T}}\tau_{\text{c}} = 2r_{\text{s}}^2/9$, where r_{s} is the sphere radius.[13] For a homogeneous lattice, $D_{\text{T}}\tau_{\text{c}} = {}^1/_{18}$ in our simulations, consistent with the choice that r_{s} equals half of the lattice spacing; i.e., the molecular diameter equals the lattice spacing.

Reorientation on a Heterogeneous Lattice. We need to calculate the rotational correlation time τ_{c} in order to construct $D_{\text{T}}\tau_{\text{c}}$. For this calculation, we have assumed that the reorientation of a molecule on the lattice is completely controlled by the local rotation time τ of one lattice site. Thus, for a static lattice ($\tau_{\text{ex}} = \infty$), we calculate the rotational correlation function as

$$\text{CF}(t) = \int_0^\infty \text{e}^{-t/\tau}\, g(\tau)\, \text{d}\tau \tag{5}$$

The rotational correlation time is always given as

$$\tau_{\text{c}} = \int_0^\infty \text{CF}(t)\, \text{dt} \tag{6}$$

For a static lattice, this simplifies to

$$\tau_{\text{c}} = \int_0^\infty \tau g(\tau)\, \text{d}\tau \tag{7}$$

When the lattice is dynamic ($\tau_{\text{ex}} < \infty$), we need to account for the possibility that the local rotation time will change before the molecule has completely lost its orientation. Consider the extreme case where several changes in the local rotation time occur prior to complete loss of orientation. In particular, imagine that a site is characterized by τ_1 between time 0 and t_1, by τ_2 between t_1 and t_2, etc. The rotational correlation function for this site is taken to be

$$\begin{aligned} \text{CF}(t) &= \text{e}^{-t/\tau_1} \qquad \text{for } 0 < t < t_1 \\ &= \text{e}^{-t_1/\tau_1}\, \text{e}^{-(t-t_1)/\tau_2} \qquad \text{for } t_1 < t < t_2 \\ &\text{etc.} \end{aligned} \tag{8}$$

By stochastically averaging over all possible time histories, the average CF(t) for the dynamic lattice can be obtained. This CF(t), described numerically using 4000 evenly spaced time points, was then characterized by fitting with the KWW equation (eq 1). The β parameter and the correlation time are designated β(sim) and τ_{c}(sim). The rotational correlation time is calculated according to the general relationship for the KWW function:

$$\tau_c = \frac{\tau}{\beta}\Gamma(1/\beta) \tag{9}$$

III. Two State Systems

We first consider a lattice in which only two dynamical states are possible. As shown below, the agreement between simulation and effective medium theory for two state systems is excellent. This result gives us further confidence that our simulation algorithm provides an accurate solution for model heterogeneous systems of the type depicted in Figure 2. Although we do not consider the two state system a physically reasonable model for dynamics in supercooled liquids, this system qualitatively illustrates enhanced translational diffusion of the type seen in recent experiments.

A two state system is specified by two local rotation times (τ_1 and τ_2), the probabilities of finding these regions (p_1 and p_2), the region size, and the average exchange time τ_{ex}. Davis used effective medium theory to give an approximate solution to this problem in the static limit ($\tau_{ex} = \infty$).[27] Zwanzig extended this calculation to variable τ_{ex}.[28] Zwanzig's solution agrees with the Davis solution in the static limit. Zwanzig and Davis described the dynamics of different regions in terms of local diffusivities, rather than local rotation times, but these descriptions are equivalent.

The long-time translational diffusion coefficient D_T is extracted from our simulation results using the following definition:

$$D_T = \lim_{t\to\infty} \frac{\langle r^2 \rangle}{6t} \tag{10}$$

(Note that Zwanzig refers to this quantity as D_{eff}, while Davis uses D_m.) Figure 3 shows the results of several simulation runs for the following conditions: $p_1 = p_2 = 1/2$, $\tau_2/\tau_1 = 100$, $\tau_2 = 1.98$, and $\tau_{ex} = \infty$. Although eq 10 suggests a plot of $\langle r^2\rangle/6t$ as a function of t, we have plotted $\langle r^2\rangle/6t$ vs $\langle r^2\rangle$ and extrapolated to large values of $\langle r^2\rangle$. This procedure also produces D_T for these systems and has the advantage that the abscissa is expressed in fundamental units of the simulation.

For each of the five runs shown in Figure 3, the large distance (long-time) portion of the plot is fairly flat, indicating that transport on these length and time scales is diffusive. Results for three different block sizes are shown in Figure 3. As expected, when the block size is smaller, the mean-square displacement needed to reach diffusive transport is also smaller. For these simulations, the root-mean-square displacement needed for $\langle r^2\rangle/6t$ to be within 10% of its long-time value is 3−4 block lengths. The D_T value predicted by the effective medium theory for this case is 0.76, independent of block size. Clearly the simulation results for all three block sizes are consistent with this prediction.

Table 1 shows D_T values obtained from simulations of static two state systems with $p_1 = p_2 = 1/2$. There is no significant effect of block size on the simulation calculation; this is reassuring since no size effect is predicted by the theory in the static limit. The agreement between the Davis/Zwanzig effective medium theory (labeled "EMT") and the simulation results is excellent for all cases investigated. The final column in Table 1 shows the product $D_T\tau_c$ for these two state simulations. Clearly this product is enhanced by orders of magnitude as the lattice becomes more heterogeneous.

Table 2 shows D_T values obtained for two state systems in which the exchange time is varied while the heterogeneity (τ_2/τ_1) is held constant. For these calculations, the individual values of t_{ex} were selected from an exponential distribution (i.e., β_{ex} = 1). D_T values calculated from Zwanzig's theory are also shown (eq 12 of ref 28). Zwanzig's theory assumes that the local regions in the heterogeneous system are spherical as opposed to the cubic regions used in the simulations. We have set the sphere radius equal to half the length of a block edge in these calculations. Rotational correlation times τ_c were calculated stochastically using the simulation parameters described in section II.

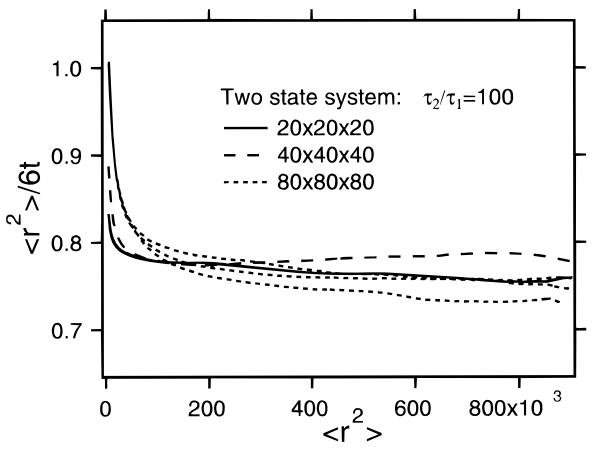

Figure 3. Results from simulations of two state systems with various block sizes. For these simulations, $p_1 = p_2 = 1/2$, $\tau_2/\tau_1 = 100$, $\tau_2 = 1.98$, and $\tau_{ex} = \infty$. At large distances, $\langle r^2\rangle/6t$ becomes constant and equal to the diffusion coefficient D_T. For these conditions, D_T is independent of the block size and consistent with the value predicted by effective medium theory. Each line represents the average of 2000 independent walks.

TABLE 1: D_T Values for Static ($\tau_{ex} = \infty$) Two State Systems with $p_1 = p_2 = 1/2$[a]

τ_2/τ_1	block size	D_T(sim)	D_T(EMT)	$D_T\tau_c$(sim)
1	20	0.056 ± 0.001	0.0555	0.056
10	20	0.127 ± 0.005	0.122	0.127
100	20	0.77 ± 0.03	0.76	0.77
	40	0.78 ± 0.03	0.76	0.78
	80	0.77 ± 0.03	0.76	0.77
1000	20	7.4 ± 0.3	7.0	7.4
	40	7.2 ± 0.3	7.0	7.2
	80	7.1 ± 0.3	7.0	7.1
	160	6.9 ± 0.3	7.0	6.9

[a] In all cases, $\tau_c = (\tau_1 + \tau_2)/2$ is constrained to be unity.

TABLE 2: D_T Values for Two State Systems with Various Values of τ_{ex}[a]

τ_{ex}	D_T(sim)	D_T(EMT)	τ_c(sim)	$D_T\tau_c$(sim)
∞	0.78 ± 0.03	0.76	1.0	0.78
100	1.03 ± 0.03	1.05	0.99	1.02
10	1.24 ± 0.04	1.25	0.91	1.13
1	1.35 ± 0.04	1.36	0.52	0.70
0.1	1.38 ± 0.04	1.40	0.13	0.18
0		1.42	0.039	0.056[b]

[a] In all cases, $\tau_2/\tau_1 = 100$ ($\tau_2 = 1.98$) and $p_1 = p_2 = 1/2$. Block size is 40 × 40 × 40. [b] Calculated from D_T(EMT).

The results in Table 2 again indicate excellent agreement between the effective medium theory and our simulations for these two state systems. As τ_{ex} decreases, D_T increases. The physical basis for this is easily understood. When τ_{ex} is very large, molecules in slow blocks must diffuse out of their current block before they have a chance to translate rapidly through a fast block. As τ_{ex} becomes smaller, the exchange process intervenes and allows molecules in slow blocks to become fast without taking the time to diffuse to a new region. In the limit that $\tau_{ex} \to 0$, it is easily shown[29] for a two state system that

$$D_T = \langle D_i \rangle \quad (11)$$

where D_i is the local diffusivity ($=1/(18\tau_i)$ in our simulations). For the simulation results shown in Table 2, eq 11 predicts $D_T = 1.42$. The effective medium theory also predicts this result, and the simulation results approach this limit.

While D_T is maximized in the limit that $\tau_{ex} \rightarrow 0$, the product $D_T\tau_c$ is not. The reason for this is that τ_c decreases as τ_{ex} decreases. The molecules which are "liberated" from slow regions by the exchange process lose their orientation faster than they would in the absence of exchange. In the limit that $\tau_{ex} \rightarrow 0$, $D_T\tau_c$ equals its value for a homogeneous lattice. Thus, in general, the conditions needed to produce eq 11 do not necessarily produce enhanced translational diffusion. Various workers attempting to explain enhanced translational diffusion have used eq 11 as an approximation under conditions where its accuracy has not been tested.[12,13,21]

IV. KWW Distributions of Local Rotation Times

We now consider the case where the local rotation time distribution is given by a KWW distribution function. This case may be relevant since the KWW distribution is often used to describe relaxation functions in supercooled liquids. As noted above, eq 11 is sometimes used as an approximate expression for the diffusion coefficient in a heterogeneous medium. This approximation is particularly bad for the KWW distribution. If the local diffusivities are taken to be inversely related to the local rotation times, as in our simulations, then eq 11 indicates that D_T should be proportional to $\langle 1/\tau \rangle$. Since this quantity diverges for the KWW distribution of rotation times for all $\beta < 1$,[30] eq 11 is clearly not useful for this case. Our simulations provide the first indications of how translational diffusion is averaged in a spatially heterogeneous system with a KWW distribution of relaxation times.

We denote the KWW parameters needed to specify the local rotation time distribution $g(\tau)$ as τ_{local} and β_{local}. $g(\tau)$ for the KWW equation with various values of β were obtained numerically at increments of 0.1 in log time. This was done using Mathematica to evaluate eq 25 of ref 30.

Static KWW Distribution. Plots of $\langle r^2 \rangle/6t$ are shown in Figure 4 for static ($\tau_{ex} = \infty$) KWW distributions with $0.3 \leq \beta \leq 0.9$. As β decreases, larger and larger mean-square displacements are required before $\langle r^2 \rangle/6t$ reaches its asymptotic limit (D_T). Diffusion coefficients are presented in Table 3. Only one block size was investigated in these simulations of static KWW distributions, but the results are not expected to depend upon block size since no size dependence is seen for two state systems in the static limit.

Table 3 also presents rotational correlation times calculated for the KWW distribution using eq 9. The final column of the table presents the logarithm of $D_T\tau_c$ normalized to the value obtained for a homogeneous matrix. These values are plotted as the solid circles in Figure 5. A line has been fit to these points and is reproduced in Figure 1. Although static spatial heterogeneity increases $D_T\tau_c$ by 5 orders of magnitude as β approaches 0.2, the enhancement is generally not as large as that observed experimentally. This comparison is not discouraging, however, since the static limit is not physically reasonable for an ergodic system and because we anticipate larger values of $D_T\tau_c$ when exchange is allowed (in analogy to Table 2).

A comparison between the simulation results and the effective medium theory of Davis (eq 6 of ref 27) is also presented in Table 3. The Davis theory was derived for systems with multicomponent static heterogeneity. As shown in the table, substantial disagreement exists between the theory and simulation results when $\beta \leq 0.7$. The magnitude of this disagreement is larger than the estimated error associated with the simulation. We ascribe the disagreement to inaccuracy of the theory. This result is surprising considering the accuracy of the effective medium theory for two state systems (Table 2). Simulations using a log Gaussian distribution of relaxation times (not reported here) also disagreed with effective medium predictions when the distribution was broad.

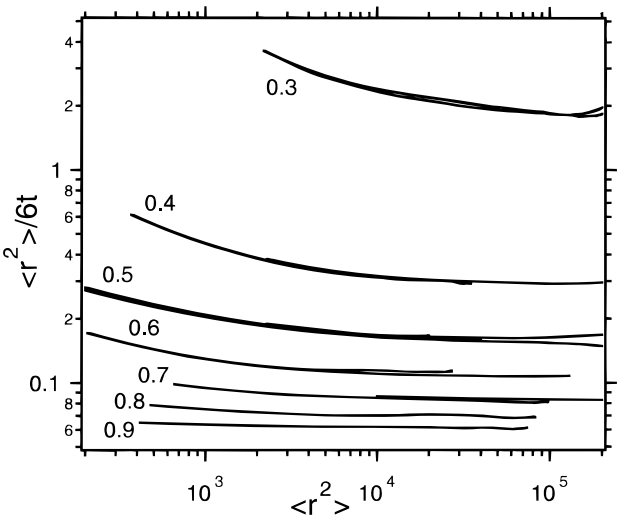

Figure 4. $\log \langle r^2 \rangle/6t$ vs $\log \langle r^2 \rangle$ for static KWW distributions of local rotation times. Results are shown for β values between 0.3 and 0.9. The block size in these simulations was $20 \times 20 \times 20$.

TABLE 3: D_T Values for Static KWW Distribution of Local Rotation Times[a]

β_{local}	D_T(sim)	D_T(EMT)	τ_c	$D_T\tau_c$(sim)	$\log[(D_T\tau_c)_{sim}/(D_T\tau_c)_{homo}]$
1.0	0.055	0.0555	1.00	0.055	0
0.9	0.062	0.0603	1.05	0.065	0.07
0.8	0.070	0.0662	1.13	0.079	0.15
0.7	0.082	0.0754	1.27	0.104	0.27
0.6	0.107	0.090	1.5	0.161	0.46
0.5	0.160 ± 0.015	0.117	2.0	0.32	0.76
0.4	0.30 ± 0.03	0.172	3.32	1.00	1.25
0.3	1.8 ± 0.3	0.473	9.26	17	2.48
0.2	100 ± 15	6.51	120	1.2×10^4	5.33

[a] In all cases $\tau_{local} = 1$, $\tau_{ex} = \infty$, and the block size is $20 \times 20 \times 20$.

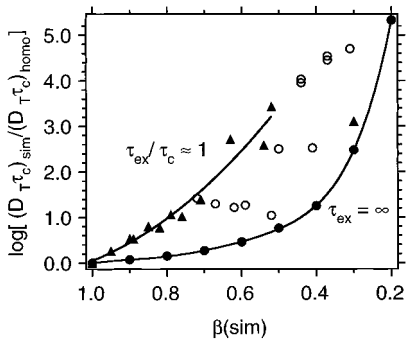

Figure 5. Simulation results for KWW distributions of local rotation times with and without exchange: no exchange, $\tau_{ex} = \infty$ (solid circles); $\tau_{ex}/\tau_c \approx 1$ (solid triangles); $1 < \tau_{ex}/\tau_c < \infty$ (open circles). The abscissa characterizes the shapes of the rotational correlation functions obtained from the simulations, while the ordinate shows the number of decades that translational diffusion is enhanced. The two solid lines are fits to the results for no exchange, and $\tau_{ex}/\tau_c \approx 1$. These lines are reproduced with experimental data in Figure 1.

TABLE 4: D_T Values for Dynamic KWW Distributions of Local Relaxation Times[a]

β_{local}	τ_{ex}	β_{ex}	D_T(sim)	τ_c(sim)	β(sim)	$\log[(D_T\tau_c)_{sim}/(D_T\tau_c)_{homo}]$	fit quality[b]
0.9	1.05	1	0.102	0.98	0.95	0.26	1
0.8	1.13	1	0.19	0.98	0.90	0.53	1
0.8	1.13	0.9	0.19	0.98	0.89	0.53	1
0.7	1.27	1	0.34	1.02	0.85	0.80	0.9
0.7	1.27	0.8	0.33	0.99	0.82	0.77	1
0.6	1.5	1	0.59	1.07	0.79	1.06	0.85
0.6	1.5	0.8	0.57	1.03	0.76	1.02	1
0.5	100	1	0.31	1.98	0.52	1.04	1
0.5	10	1	0.60	1.72	0.59	1.27	0.85
0.5	2	1	1.21	1.20	0.72	1.42	0.8
0.5	2	0.7	0.98 ± 0.15	1.13	0.67	1.30	0.9
0.5	2	0.5	0.88 ± 0.15	1.06	0.62	1.22	1
0.5	1	0.7	1.46	0.93	0.71	1.39	0.85
0.3	20	0.5	5.4 ± 1	3.4	0.41	2.52	0.7
0.3	2	0.5	14 ± 2	1.25	0.50	2.50	0.7
0.3	1	0.7	30 ± 5	0.94	0.63	2.71	0.65
0.3	1	0.5	25 ± 4	0.84	0.54	2.58	0.7
0.2	200	0.5	115 ± 15	24	0.31	4.70	0.4
0.2	50	0.5	130 ± 30	12	0.37	4.45	0.4
0.2	5	0.5	180 ± 30	2.8	0.44	3.95	0.5
0.2	0.5	0.5	290	0.52	0.52	3.43	0.6
0.2	0.5	0.2	205 ± 20	0.34	0.30	3.10	0.8

[a] $\tau_{local} = 1$ for all simulations. Block size equals $20 \times 20 \times 20$. [b] The simulated CF(t) is well described by β(sim) and τ_c(sim) for values of CF(t) less than the value given.

KWW Distribution with Exchange. We expect that these simulations are the most reasonable physically since a continuous distribution of relaxation times is utilized along with exchange processes which allow the system to be ergodic. Table 4 presents the results of simulations using KWW distributions with exchange. To make our results as clear as possible, we begin by reviewing the three different ways we have used KWW equations/distributions in this paper: (1) Two parameters characterize the distribution of local rotation times, τ_{local} and β_{local} (τ_{local} is set equal to unity in these simulations). (2) Two parameters specify the exchange process, τ_{ex} and β_{ex}. The local rotation times of the blocks are exchanged every τ_{ex}, on average. The individual exchange times t_{ex} are selected from a distribution such that the probability of selecting a particular t_{ex} decays as a stretched exponential characterized by β_{ex}. (3) As noted in section II, when $\tau_{ex} < \infty$, the rotational correlation function CF(t) predicted from the simulation (eq 8) is not characterized by τ_{local} and β_{local}. The simulated CF(t) is characterized by β(sim) and τ_c(sim).

Our first simulations with the dynamic KWW distribution utilized an exponential distribution of exchange times; i.e., $\beta_{ex} = 1$. We discovered that the rotational correlation functions which resulted were not fitted well by the KWW equation. Figure 6 illustrates this for one example. The initial decay of the correlation function is described by τ_{local} and β_{local} (dashed line). Since τ_{ex} is small, the long-time portion of the function is cut off by exchange. The best KWW fit to the simulated function is shown by the solid line and has β(sim) > β_{local}. Clearly this fit is not good for CF(t) > 0.8. The fit quality for all of the simulated correlation functions is indicated in the final column of the Table 4. The fit to CF(t) is good for values of CF(t) less than the listed value. Thus, for the example shown in Figure 6, the fit quality column reads 0.8.

When a KWW distribution of exchange times was used, the resulting correlation functions were better fit by the KWW equation. This trend can be illustrated by the three simulations listed in Table 4 for which $\beta_{local} = 0.5$ and $\tau_{ex} = 2$. When β_{ex} is decreased from 1 to 0.5, the KWW fit is essentially perfect. These three simulations also illustrate another important trend. As β_{ex} increases, enhanced translation becomes more pronounced, mainly because β(sim) increases. Thus, a tradeoff exists between the quality of the fits to the rotational correlation function and the apparent enhancement of translational diffusion. This tradeoff is even more dramatic for the two simulations with $\beta_{local} = 0.2$ and $\tau_{ex} = 0.5$.

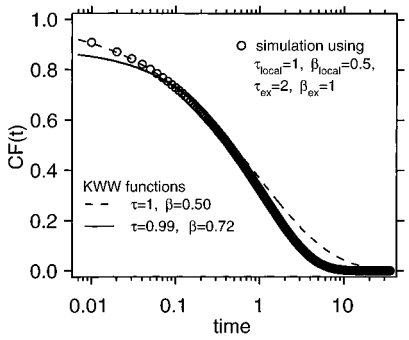

Figure 6. Effect of exchange on the rotational correlation function. In the absence of exchange, the simulation results would follow the dashed line at all times. Exchange has no effect on the initial part of the correlation function decay but cuts off the tail of the function. Physically this occurs because, on average, exchange shortens the rotation times of molecules which otherwise would have rotated very slowly. The simulated correlation function with exchange is reasonably fit [below CF(t) = 0.8] to a KWW function with a β value larger than that which characterizes the distribution of local rotation times.

Figure 5 shows all of the results from Table 4, with solid triangles representing cases where $\tau_{ex}/\tau_c \approx 1$. Open circles represent larger values of this ratio. Enhanced translation is more pronounced for a given β as exchange occurs more rapidly. (Even more rapid exchange would eventually lead to less enhanced translation, in analogy with Table 2.) The solid line fit through the triangles represents the largest translational enhancements which result from these simulations for the condition $\tau_{ex}/\tau_c \approx 1$ (i.e., we exclude the solid triangle with β(sim) = 0.3). We reiterate that the fit to the simulated rotational correlation functions is not perfect for several of the points shown in Figure 5. In particular, this is the case for all solid triangles for which β(sim) is less than 0.75.

The upper solid line in Figure 5 has been reproduced in Figure 1 and plotted with the experimental data. All of the experimental data are consistent with this line or lie below it. Our interpretation of this is as follows. Our model system with

TABLE 5: D_T Values as a Function of Block Size for Dynamic KWW Distributions[a]

β_{local}	block size	τ_{ex}/τ_c(sim)	β_{ex}	D_T(sim)
0.5	80	1.7	1	2.8
0.5	40	1.7	1	1.8
0.5	20	1.7	1	1.21
0.2	20	8.3	0.5	115 ± 15
0.2	10	8.3	0.5	125 ± 20
0.2	5	8.3	0.5	140 ± 20
0.2	20	1.8	0.5	180 ± 30
0.2	5	1.8	0.5	165 ± 20

[a] $\tau_{local} = 1$ for all simulations.

spatially heterogeneous dynamics (Figure 2) produces enhanced translational diffusion in agreement with experimental results for values of τ_{ex}/τ_c between unity and infinity. Some of the data are only consistent with the model when $\tau_{ex}/\tau_c \approx 1$. Most of the experimental data are consistent with somewhat larger values of τ_{ex}/τ_c, perhaps as large as 6−10 or higher. The fact that the simulated rotational correlation functions are not always well-described by the KWW function does not have a significant effect on this interpretation since these short-time deviations are probably too small to have been detected in the experimental data reported in refs 11, 13, 17, 18, and 31. As discussed in these references, the photobleaching experiment used to measure the rotational correlation function is not very sensitive to dynamics at short times.

Experimental estimates of τ_{ex}/τ_c are varied and span the range of values discussed in the previous paragraph. Four-dimensional NMR experiments performed by Bohmer et al. on *o*-terphenyl at $T_g + 10$ K indicated that the time scales for reorientation and exchange are similar.[7] Optical deep bleaching experiments by Cicerone and Ediger on *o*-terphenyl at T_g indicated that the exchange time was 100−1000 times longer than the rotational correlation time.[9] Very recently dielectric hole burning experiments have been performed by Schiener et al. on propylene carbonate and glycerol at T_g.[8] These experiments indicate that exchange times are at least as long as the rotational correlation times.

All results in Table 4 were obtained using a block size of 20. The effect of block size on simulation results for selected cases is illustrated in Table 5. As expected from the two state simulations, the effect of block size is small when τ_{ex}/τ_c is large. For small values of τ_{ex}/τ_c, D_T increases as the block size increases. Physically this results from molecules traveling further in fast regions if the blocks are large. While this effect is clearly not negligible, we regard it as a second order effect in comparison to the orders of magnitude variation in the product $D_T\tau_c$. A block size of 20 corresponds to roughly 20 molecular diameters across one block and thus is slightly larger than various estimates of the important length scales for dynamic heterogeneity in supercooled liquids.

V. Concluding Remarks

We have presented simulations of a simple model of spatially heterogeneous dynamics. Translational diffusion can be enhanced by more than 5 orders of magnitude with the range of input parameters we have explored. More significantly, the simulation results produce a correlation between $D_T\tau_c$ and the β parameter which characterizes the rotational correlation function for the heterogeneous system. This correlation is similar to the one observed experimentally for several supercooled liquids near T_g. The experimental data can be reproduced by the model when the exchange time for scrambling the dynamics in a given region is 1−10 times longer than the rotational correlation time.

Clearly the model used here is simplistic and somewhat unrealistic as a description of supercooled liquids. One of the most serious assumptions made in the model is that regions of different dynamics are separated by sharp regular boundaries. We have also assumed that the dynamics are uncorrelated from region to region and that locally rotation and translation are influenced in the same way by a nearby boundary. Even so, we consider this a reasonable zero order model for transport in deeply supercooled liquids. The results presented here make a plausible argument for this. While it is easy to imagine more realistic (and computationally intensive!) models of spatially heterogeneous dynamics in supercooled liquids, we believe that this model is the most realistic one tested to date.

Given the simplicity of the model, what features of these results are likely to be robust? We speculate on two points. First, the argument that enhanced translational diffusion is caused by spatially heterogeneous dynamics is considerably strengthened by these results. Second, the results support the view that most of the non-exponentiality of the rotational correlation function is a result of spatially heterogeneous dynamics. The model assumes that spatially heterogeneous dynamics is fully responsible for non-exponential rotational correlation functions. Any other assumption would make the enhanced translation effect smaller. Since the model just barely produces a large enough enhanced translation effect as it is, the model assumption is likely close to the truth.

These simulations, and the experiments they were designed to mimic, do not specify the origin of spatially heterogeneous dynamics in supercooled liquids. Other experiments have not yet provided definitive information on this point either. Quite a number of ideas in the literature might be relevant. The idea of an increasing length scale for cooperativity in molecular motion as T_g is approached has been widely discussed,[32,33] and may explain spatially heterogeneous dynamics. Others have proposed that the dynamics are heterogeneous due to density fluctuations related to the compressibility[9] or other origins.[34−36] Still others have argued that the heterogeneity is a result of an avoided critical point.[37] Clearly additional work is required on this important issue.

Acknowledgment. The authors thank National Science Foundation (NSF) Chemistry (Grant CHE-9618824) for funding this work. We thank Jim Skinner for helpful discussions and Chia-Ying Wang for calculating $g(\tau)$ for KWW distribution. We thank Hans Sillescu, Peter Harrowell, and John Bendler for comments on the manuscript. The workstations used in this work were purchased through a grant from NSF (Grant CHE-9522057).

References and Notes

(1) Ediger, M. D.; Angell, C. A.; Nagel, S. R. *J. Phys. Chem.* **1996**, *100*, 13200.
(2) Angell, C. A. *Science* **1995**, *267*, 1924. Stillinger, F. H. *Science* **1995**, *267*, 1935, and references cited therein.
(3) See: Proceedings of the Second International Discussion Meeting on Relaxations in Complex Systems. *J. Non-Cryst. Solids* **1994**, 172−174.
(4) See for example: Bohmer, R.; Ngai, K. L.; Angell, C. A.; Plazek, D. J. *J. Chem. Phys.* **1993**, *99*, 4201.
(5) For recent insights into this issue see: Heuer, A.; Okun, K. *J. Chem. Phys. B* **1997**, *106*, 6176.
(6) Heuer, A.; Wilhelm, M.; Zimmermann, H.; Spiess, H. *Phys. Rev. Lett.* **1995**, *75*, 2851.
(7) Bohmer, R.; Hinze, G.; Diezemann, G.; Geil, B.; Sillescu, H. *Europhys. Lett.* **1996**, *36*, 55.
(8) Schiener, B.; Bohmer, R.; Loidl, A.; Chamberlin, R. V. *Science* **1996**, *274*, 752.
(9) Cicerone, M. T.; Ediger, M. D. *J. Chem. Phys.* **1995**, *103*, 5684.
(10) Moynihan, C. T.; Schroeder, J. *J. Non-Cryst. Solids* **1993**, *160*, 52.
(11) Cicerone, M. T.; Ediger, M. D. *J. Chem. Phys.* **1996**, *104*, 7210.

(12) Fujara, F.; Geil, B.; Sillescu, H.; Fleischer, G. *Z. Phys. B* **1992**, *88*, 195.
(13) Blackburn, F.; Wang, C.-Y.; Ediger, M. D. *J. Phys. Chem*. **1996**, 100, 18249.
(14) Chang, I.; Sillescu, H. *J. Phys. Chem.*, in press.
(15) Heuberger, G.; Sillescu, H. *J. Phys. Chem.* **1996**, *100*, 15255.
(16) Rossler, E.; Eiermann, P. *J. Chem. Phys.* **1994**, *100*, 5237.
(17) Cicerone, M. T.; Blackburn, F. R.; Ediger, M. D. *Macromolecules* **1995**, *28*, 8224.
(18) Hwang, Y.; Ediger, M. D. *J. Polym. Sci., Polym. Phys. Ed*. **1996**, *34*, 2853.
(19) Deppe, D. D.; Dhinojwala, A.; Torkelson, J. M. *Macromolecules* **1996**, *29*, 3898.
(20) For a related recent effort see: Liu, C. Z.-W.; Oppenheim, I. *Phys. Rev. E* **1996**, *53*, 799.
(21) Tarjus, D.; Kivelson, D. *J. Chem. Phys*. **1995**, *103*, 3071.
(22) As described in ref 13, the value of $D_T\tau_c$ expected in a homogeneous environment was calculated from the equation $(D_T\tau_c)_{homo} = 2/9r_s^2$. High-temperature rotation measurements in *o*-terphenyl were used to obtain the following values of r_s: anthracene, 1.9 Å; tetracene, 2.1 Å; BPEA, 4.7 Å; and rubrene, 4.9 Å.
(23) Shlesinger, M. F.; Montroll, E. W. *Proc. Natl. Acad. Sci. U.S.A.* **1984**, *81*, 1280.
(24) Diezemann, G. *J. Chem. Phys.*, in press.
(25) In the case of a stretched exponential, the following procedure was used. One random number was used to select a particular τ value from the distribution specified by τ_{ex} and β_{ex}. This τ was multiplied by $-\ln(x)$, where x is a second random number from the uniform distribution between 0 and 1.
(26) Bedeaux, D.; Lakatos-Linderberg, K.; Shuler, K. E. *J. Math. Phys*. **1971**, *12*, 2116.
(27) Davis, H. T. *J. Am. Ceram. Soc.* **1977**, *60*, 499.
(28) Zwanzig, R. *Chem. Phys. Lett.* **1989**, *164*, 639.
(29) See for example endnote 28 of ref 11.
(30) Lindsey, D. P.; Patterson, G. D. *J. Chem. Phys*. **1980**, *73*, 3348.
(31) Bainbridge, D.; Ediger, M. D. *Rheol. Acta*. **1997**, *36*, 209.
(32) Adam, G.; Gibbs, J. H. *J. Chem. Phys*. **1965**, *43*, 139.
(33) Donth, E. *J. Non-Cryst. Solid*s **1982**, *53*, 325.
(34) Stillinger, F. H.; Hodgdon, J. A. *Phys. Rev. E* **1994**, *50*, 2064.
(35) Moynihan, C. T.; Whang, J.-H. *Mater. Res. Soc. Symp. Proc.* **1997**, *455*, 133.
(36) Hurley, M. M.; Harrowell, P. *Phys. Rev. E* **1995**, *52*, 1694.
(37) Kivelson, D.; Kivelson, S. A.; Zhao, X.; Nussinov, Z.; Tarjus, G. *Physica A* **1994**, *205*, 738.